EPiC Series in Technology
Volume 4, 2026, Pages 57–64
Proceedings of The 11th International Conference on Tribology in Manufacturing Processes & Advanced Surface Engineering

Machine Learning Analysis of Bonding Strength and Forging Conditions in Forge-Bonding with Circumferential Sliding

Ryo Matsumoto[1,2], Kakeru Hashimoto[2] and Hiroshi Utsunomiya[2]
[1] Nagoya Institute of Technology, Aichi, Japan
[2] The University of Osaka, Osaka, Japan
matsumoto.ryo@nitech.ac.jp

Abstract

To investigate the influence of the circumferential sliding at the upper–lower workpiece contact interface on the bonding characteristics in forge-bonding with copper and aluminum workpieces, the experimental relationship between the forge-bonding conditions and the bonding characteristics was analyzed by means of machine learning analysis. The bonding probability was predicted with an accuracy of approximately 90%, while the bonding strength was predicted with an accuracy comparable to the experimental scattering. Furthermore, the circumferential sliding at the upper–lower workpiece contact interface was secondary greatest influence, following forging stroke, on both bonding probability and bonding strength.

1 Introduction

To achieve desirable mechanical and functional properties in structural components, multi-material components, designed by combining dissimilar materials, have attracted great attention. In manufacturing of the multi-material components, bonding and joining processes of dissimilar materials are crucial processes. Among joining techniques based on cold forging, forge spot-bonding process [1] and backward extrusion forge-bonding process [2,3] have been proposed. In the case of backward extrusion forge-bonding process, the dissimilar materials, stacked in the extrusion direction, was demonstrated to be simultaneously forged and bonded. On the other hand, bonding strength of dissimilar materials was reported to be enhanced by increasing a tangential relative sliding at the contact interface in cold pressure welding [4]. Furthermore, the increase of relative sliding at the contact interface was reported to reduce the minimum reduction in thickness for bonding of the stacked sheets in cold differential speed rolling [5]. Based on these findings, we proposed a cold forge-bonding process with circumferential sliding [6]. The circumferential sliding shortened the forging stroke for bonding by approximately 25% and increased the bonding strength by four times at the same forging stroke in cold copper/aluminum forge-bonding. The improvement in bonding characteristics by applying circumferential sliding was mainly due to the increase of adhesion of the aluminum workpiece on the copper workpiece.

Incidentally, machine learning techniques have dramatically expanded to be applied in the field of metal forming. For example, recognition of forming state of sheet in deep drawing [7], generation of tool path in incremental sheet forming [8], and analysis of forming behavior in cold forging [9] have been addressed through neural network (NN) techniques. On the other hand, factor analysis of dimensional scattering of extruded products in extrusion process has been reported by means of Lasso regression and random forest [9].

In this study, to investigate the influence of the circumferential sliding at the upper–lower workpiece contact interface on the bonding characteristics in forge-bonding with copper and aluminum workpieces, the experimental relationship between the forge-bonding conditions and the bonding characteristics was analyzed by means of machine learning analysis. The bonding strength and probability were predicted by means of random forest. The influence of the circumferential sliding on the bonding characteristics is discussed from the feature importances of each forge-bonding process parameter.

2 Experimental Conditions of Backward Extrusion Forge-Bonding with Circumferential Sliding

Figure 1 shows the schematic illustrations of the layout of dies and workpieces, and the forged workpieces in backward extrusion forge-bonding with circumferential sliding. Two cylindrical workpieces with same diameter stacked in forging direction (z direction) were located on the lower (knockout) punch inserted in the container. The upper (extrusion) punch was moved in the -z direction for backward extrusion of the workpieces. Simultaneously the lower punch was rotated in the circumferential direction (θ direction) with respect to the z-axis. Owing to the knurled grooves on the end faces of the upper and lower punches, no sliding occurred at the both contact interfaces of the end face of the upper punch–top of the upper workpiece and the end face of the lower punch–bottom of the lower workpiece. On the other hand, sliding occurred in the circumferential direction at the upper–lower workpiece contact interface.

The upper and lower workpieces were JIS C1100-O copper (> 99.90 mass% Cu, 73 HV0.2) and JIS A1070-O aluminum (> 99.70 mass% Al, 37 HV0.2), respectively. The initial shape of the upper workpiece was cylindrical with a diameter of $d_{u0} = \phi 13.9$ mm and a height of h_{u0} = 4–6 mm, while that of the lower workpiece was cylindrical with a diameter of $d_{l0} = \phi 13.9$ mm and a height of h_{l0} = 6–8 mm. The total initial height of the initial upper and lower workpieces was set to $h_{u0}+h_{l0}$ = 12 mm. To remove the oxide film at the upper–lower workpiece contact interface, the bottom surface of the upper workpiece and the top surface of the lower workpiece were polished with #400 emery paper under wet condition just before forge-bonding. The arithmetic mean surface roughness of the workpieces was Ra = 0.40–0.60 μm on the end face after polishing.

Dies were made of JIS SKH51 high-speed tool steel (63 HRC). Both diameters of the lower punch and the inner diameter of the conainer were ϕ14.0 mm. The diameter of the upper punch was d_p = ϕ5.0–ϕ9.0 mm, and the extrusion ratio was set to 1.15–1.70. Mineral oil with a kinematic viscosity of 32 mm^2/s at a temperature of 313 K was applied on the inner diameter of the container before forge-bonding.

The basic forge-bonding conditions were set to h_{u0} = 5 mm, h_{l0} = 7 mm, d_p = ϕ9.0 mm (extrusion ratio: 1.70). The upper punch speed was set to 0.1 mm/s with the stroke of s = 0–9.1 mm in the -z direction, while the lower punch rotation rate and angle were set to ω = 0–2.0 rpm and θ_{cum} = 0–590°

with respect to the z-axis. Forge-bonding was carried out at room temperature. The details of the experimental conditions were shown in our previous report [6].

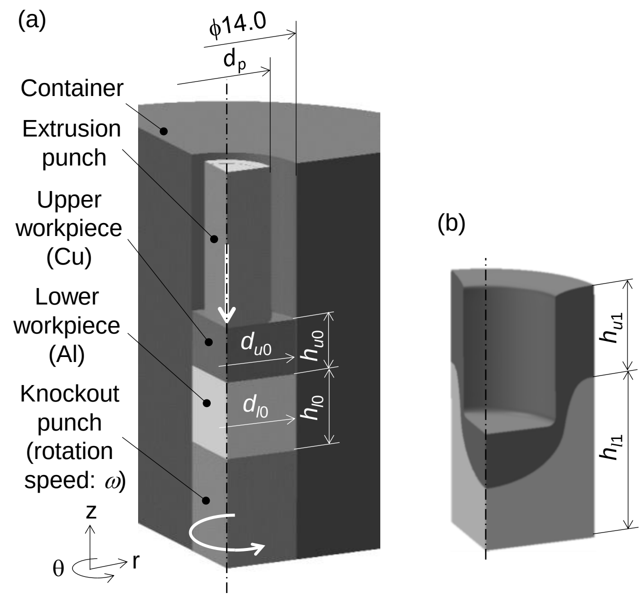

Figure 1: Schematic illustrations (quarter longitudinal section) of (a) layout of dies and workpieces and (b) forged workpieces (forging stroke s = 5.0 mm) in backward extrusion forge-bonding with circumferential sliding.

3 Machine Learning Conditions

3.1 Analysis Data

In backward extrusion forge-bonding with circumferential sliding, the experimental data with 94 conditions (58: bonding, 36: no bonding) and the pseudo data with 22 conditions (22: no bonding), resulting in a total of 116 data were used for data analysis. To eliminate the influence of our experimental knowledge for forge-bonding on the analysis results, all processing parameters (12 variables) set and measured in the forge-bonding experiment were treated as explanatory variables. The processing variables used as the explanatory variables are shown in Table 1. Here, s, ω, d_p, h_{u0}, h_{l0}, d_{u0}, and d_{l0} were the primary variables set prior to the forge-bonding experiment, while θ_{cum} was determined by s and ω. The others were the secondary data obtained either during or after the forge-bonding experiment. Furthermore, each explanatory variable was standardized (mean: 0, variance: 1), and the target variable was defined as either the bonding state (bonding, no boding) or the bonding strength.

Table 1: Explanatory variables for machine learning.

Feature	Abbreviation
Axial stroke of extrusion punch /mm	s
Rotation rate of knockout punch /rpm	ω
Diameter of extrusion punch /mm	d_p
Heights of initial upper and lower workpieces /mm	h_{u0}, h_{l0}
Diameters of initial upper and lower workpieces /mm	d_{u0}, d_{l0}
Cumulative rotation angle of knockout punch /º	θ_{cum}
Maximum axial load /MPa	F_{max}
Maximum torque /N·m	T_{max}
Sidewall height of forged upper workpiece /mm	h_{u1}
Height of forged lower workpiece /mm	h_{l1}

3.2 Analysis Conditions

The open-source library scikit-learn (ver. 0.23.1) [11] was employed for machine learning of the data analysis. A program code was developed in Python ver. 3.7.4 to execute the input, standardization, library integration, and output of the analysis results of the forge-bonding experimental data. The predictions of the bonding state (bonding, no boding) and the bonding strength were carried out by means of random forest, and the relative importance of each explanatory variable on the response variable was quantified. For the prediction of the bonding strength, the accuracy of the prediction was estimated by the coefficient of determination (R^2) and the root mean square error (RMSE), as expressed by the following equations.

$$R^2 = 1 - \frac{\sum_{i=1}^{n}\left(y_{exp,i}-y_{pred,i}\right)^2}{\sum_{i=1}^{n}\left(y_{exp,i}-\bar{y}_{exp}\right)^2} \tag{1}$$

$$RMSE = \sqrt{\frac{\sum_{i=1}^{n}\left(y_{exp,i}-y_{pred,i}\right)^2}{n}} \quad \text{[MPa]} \tag{2}$$

Here, $y_{exp,i}$, $\bar{y}_{exp}$, and $y_{pred,i}$ were the input values of the bonding strength, the mean of the input values, and the predicted values, respectively, while n was the number of data in the training and validation datasets.

In the prediction of the bonding strength by means of the random forest, 81 out of 116 forge-bonding experimental conditions were employed as training data, while the others (35 conditions) were used as validation data. Through cross-validation, the number of decision trees and the depth of the random forest were set to 1000 trees and less than 10 layers, respectively.

4 Analysis Results and Discussions

4.1 Bonding Strength

Figure 2 shows the experimental and predicted relationships between bonding strength and basic forge-bonding conditions (h_{u0} = 5 mm, h_{l0} = 7 mm, d_p = ϕ9 mm). Here, the bonding strength was predicted from the forge-bonding conditions plotted as the solid circles in Figure 2. The prediction accuracy was slightly low under forge-bonding conditions associated with high bonding strength (long forging stroke and large rotation angle). In the experimental results, forging-bonding conditions exhibiting locally high or low joint strength were regarded as outliers. However, these outliers were averaged in the predicted joint strength, yielding comparatively smooth contour lines in Figure 2. This is because the multidimensional correlations among the forge-bonding conditions were considered in the prediction of the bonding strength by the random forest.

Figure 3 shows the bonding probability under basic forge-bonding conditions. Here, the bonding probability was predicted from the forge-bonding conditions plotted as the solid circles in Figure 3. As the experimental relationship (Figure 2(a)) and the estimated results exhibited the similar tendency, the random forest was indicated to be effective for the prediction of the bonding probability. Based on the results under basic forge-bonding conditions, the prediction of the bonding probability using the random forest were conducted for all forge-bonding conditions (116 conditions). The bonding probability of higher than 50% was determined to be "bonding", while that of lower than 50% was determined to be "no bonding". The prediction accuracy was 100% for the training data (81 conditions) and 91.4% for the validation dataset (35 conditions). As long as the conditions within the experimental range, the bonding probability under untested forge-bonding conditions is concluded to be predicted with high accuracy by this analysis method.

The comparison between the experimental and predicted bonding strength under all forge-bonding conditions is shown in Figure 4. *RMSE* for the training data (81 conditions) and the validation data (35 conditions) were 2.3 MPa and 4.5 MPa, respectively. Since the maximum standard deviation of the experimental bonding strength was σ = 3.1 MPa (s = 7 mm, ω = 0.5 rpm), *RMSE* for the validation data (4.5 MPa) can be regarded as reasonable. The standard deviation of the experimental bonding strength depended on the forge-bonding conditions, and it is expected that the standard deviation tends to be large under forge-bonding conditions with high bonding strength. This tendency is further suggested by Figure 4(b), which shows that prediction accuracy decreased as bonding strength increased. To enhance the prediction accuracy, it would be effective to measure the bonding strength under wider range of forge-bonding conditions and incorporate these data into the training dataset.

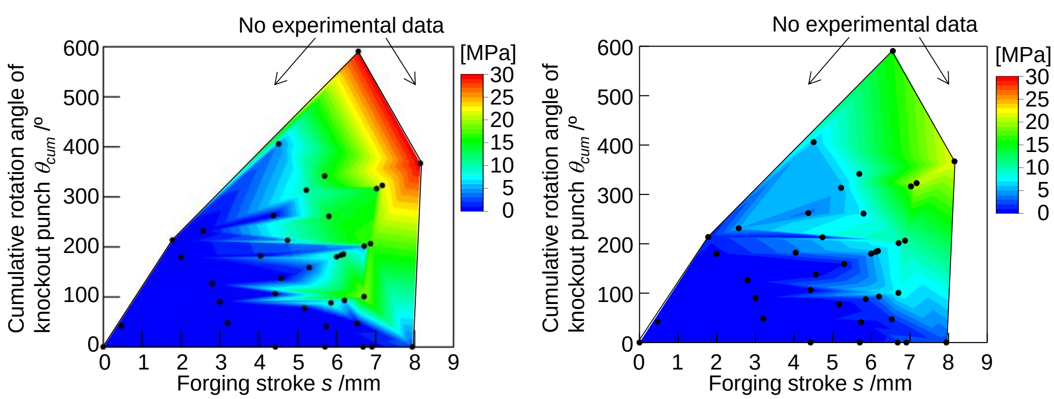

(a) Experimental results. (b) Predicted results.

Figure 2: Bonding strength of forge-bonded workpiece under basic forge-bonding conditions (h_{u0} = 5 mm, h_{l0} = 7 mm, d_p = ϕ9.0 mm) (solid circles: input experimental relationship for prediction).

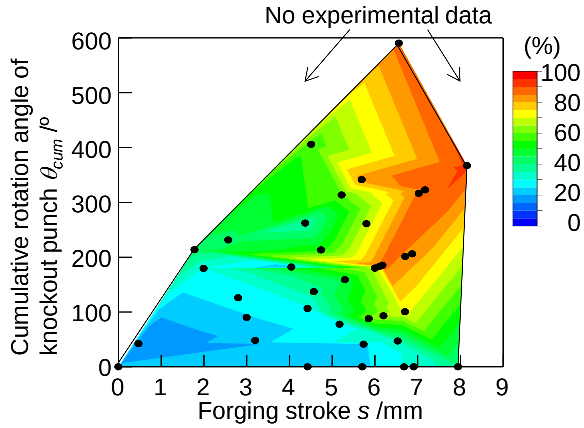

Figure 3: Bonding probability of forge-bonded workpiece under basic forge-bonding conditions (solid circles: input experimental relationship for prediction).

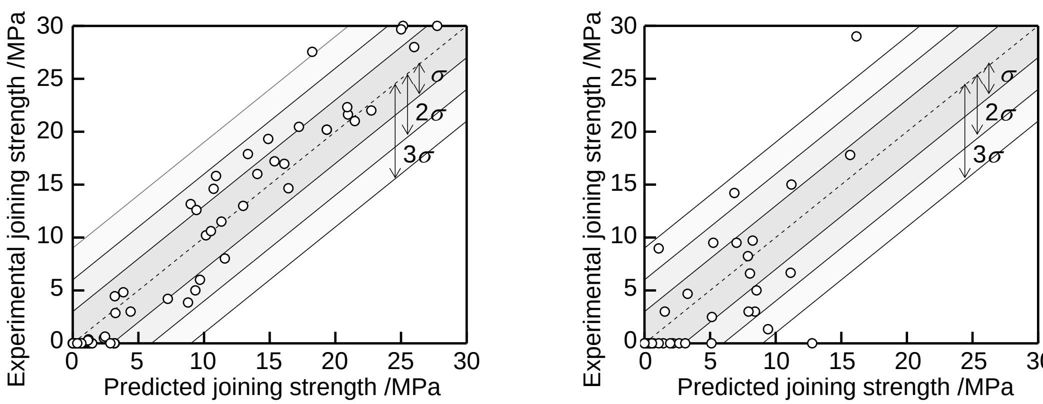

(a) Training data (R^2 = 0.93, *RMSE* = 2.3 MPa).

(b) Validation data (R^2 = 0.51, *RMSE* = 4.5 MPa).

Figure 4: Comparison between experimental and predicted bonding strength of forge-bonded workpiece under all forge-bonding conditions (standard deviation of bonding strength in experiment: σ = 3.1 MPa).

4.2 Feature Importance

Figure 5 shows the feature importances of each explanatory variable in relation to the bonding probability and the bonding strength. In both cases, the variables of s and θ_{cum} exhibited high feature importance. This indicates that the increases of s and θ_{cum} can enhance the bonding strength. In addition, since the feature importances of θ_{cum} and s were comparable, this implies that the application of the circumferential sliding on the upper–lower workpiece contact interface has an effect on enhancing the bonding strength equivalent to that of the increase of the forging stroke. However, in forge-bonding experiment, an excessive increase in the circumferential sliding may induce (a) the delamination at the bonding interface due to stick–slip phenomena and (b) torsional fracture of the workpiece.

On the other hand, the feature importances of the initial workpiece dimensions, namely h_{u0}, h_{l0}, d_u, and d_{l0}, were overall low. The influence of the initial height ratio of the upper and lower workpieces on the bonding probability and the bonding strength was concluded to be small in these forge-bonding conditions. Likewise, the feature importance of d_p was also low, suggesting that sufficient contacting pressure was applied to the upper–lower workpiece contact interface during forge-bonding with all extrusion ratios.

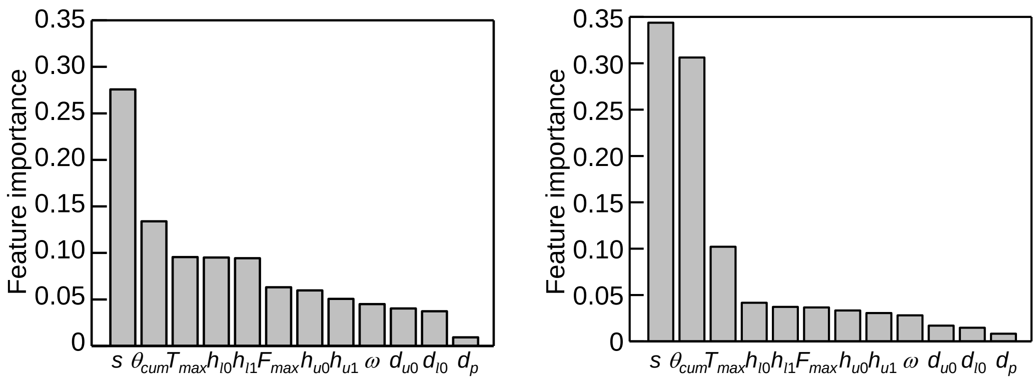

(a) For bonding probability. (b) For bonding strength.

Figure 5: Feature importances of each explanatory variable in forge-bonding with circumferential sliding.

5 Conclusions

In this study, machine learning analysis was carried out to the experimental relationship between the forge-bonding conditions and the bonding characteristics in forge-bonding with circumferential sliding. The bonding probability was predicted with an accuracy of approximately 90%, while the bonding strength was predicted with an accuracy comparable to the experimental scattering. Furthermore, the application of the circumferential sliding to the upper–lower workpiece contact interface was secondary greatest influence, following forging stroke, on both bonding probability and bonding strength. Thus the effective of the circumferential sliding on the bonding characteristics was confirmed from a viewpoint of data-driven analysis.

Acknowledgement

This study was financially supported in part by the Amada Foundation (AF-2025001-A3).

References

[1] Y. Miwada, T. Ishiguro, E. Abe, N. Yukawa, T. Ishikawa, T. Suganuma, "Cold forge spot-bonding of high tensile strength steel and aluminum alloy sheets," *Procedia Engineering*, vol. 81, pp. 2006-2011, 2014.

[2] Y. Yoshida, T. Matsubara, K. Yasui, T. Ishikawa, T. Suganuma, “Influence of processing parameters on bonding conditions in backward extrusion forged bonding,” *Key Engineering Materials*, Vols. 504-506, pp. 387-392, 2012.

[3] P. Groche, S. Wohletz, A. Erbe, A. Altin, “Effect of the primary heat treatment on the bond formation in cold welding of aluminum and steel by cold forging,” *Journal of Materials Processing Technology*, Vol. 214, No. 10, pp. 2040-2048, 2014.

[4] O. Ohashi, T. Hashimoto, “The effects of sliding along interface and anodic oxidation on cold welding of aluminum-aluminum and aluminum copper,” *Journal of the Japan Welding Society*, Vol. 47, No. 5, pp. 294-299, 1978.

[5] M. Nakamura, S. Maki, T. Matsuda, N. Nagai, “Cold bonding of metal sheets using mutual sliding by modified contact differential speed rolling,” *Journal of the Japan Society for Technology of Plasticity*, Vol. 29, No. 327, pp. 404-410, 1988.

[6] R. Matsumoto, K. Hashimoto, H. Utsunomiya, “Improvement in bonding strength by applying circumferential sliding in cold copper/aluminum forge-bonding”, *Journal of Materials Processing Technology*, Vol. 307, 117685, 2022.

[7] T. Tsuruya, M. Danseko, K. Sakaki, S. Honda, R. Takeda, “Forming state recognition in deep drawing process with machine learning,” *Journal of Advanced Mechanical Design, Systems, and Manufacturing*, Vol. 13, No. 3, 19-00205, 2019.

[8] M. Otsu, S. Yoshida, T. Miura, “Generation of tool path in incremental forming by neural network,” *Proceedings of the JSME International Conference on Materials and Processing (ICM&P 2022)*, Tu-2C-3, 2022.

[9] P.M. Petkar, V.N. Gaitonde, S.R. Karnik, V.N. Kulkarni, T.K.G. Raju and J.P. Davim, “Analysis of forming behavior in cold forging of AISI 1010 steel using artificial neural network,” *Metal*, Vol. 10, 1431, 2020.

[10] C. Sasaki, K. Kuriki, Y. Zhenmi, H. Kito, S. Hayakawa, T. Hakoyama, Z.G. Wang, “Examination of factor analysis method of dimensional variation by machine learning,” *Proceedings of the 71st Japanese Joint Conference for the Technology of Plasticity*, pp. 47-48, 2020.

[11] F. Pedregosa, G. Varoquaux, A. Gramfort, V. Michel, B. Thirion, O. Grisel, M. Blondel, P. Prettenhofer, R. Weiss, V. Dubourg, J. Vanderplas, A. Passos, D. Cournapeau, M. Brucher, M. Perrot, E. Duchesnay, “Scikit-learn: machine learning in Python,” *Journal of Machine Learning Research*, Vol. 12, No. 85, pp. 2825-2830, 2011.